Morphology Distribution and Processing History of Injection Moulded Polypropylenes

Guangwei Liu, Peng Wei Zhu and Graham Edward *

CRC for Polymers, School of Physics and Materials Engineering, Monash University, Clayton, Victoria 3800, Australia

Summary: The morphology distribution of injection moulded polypropylenes observed using optical microscopy and synchrotron X radiation is reported, the mouldings being performed under a range of conditions and with different grades of polypropylene. As has been observed before, a three-region multi-layer model is generally sufficient at first sight to describe the skin-core morphology of these injection-molded parts, with a surface skin, a spherulitic core and a transition shear layer. However the detail obtained using the high spatial resolution of the synchrotron X radiation reveals an underlying complexity. Samples were taken from PP plates at different distances from the end gate of the linear mouldings, and the X-ray data used to determine the distributions of crystallinity, β-phase concentration and the long spacing of crystallites. Different distributions are observed at different distances from the gate. The simulation software package Moldflow MPI, together with a simplified particle-tracking model is used to predict the thermal and shear histories of the polymer melt during the injection moulding process. The features of the layered structure and their dependence on the thermal and shear histories are discussed.

Introduction

The morphology of injection moulded semicrystalline polymers is a skin-core structure[1-3] in which multiple layers have been observed. The layer numbers may vary from one semicrystalline polymer to another and the structures are markedly dependent on moulding conditions, including cavity thickness, mould temperature, injection speed and pressure, holding pressure, and cooling time. For injection-moulded iPP, at least three different regions are observed through the thickness when thin sections of mouldings are examined using optical microscopy. It is possible that a more detailed examination could lead to the assignation of more layers but the definition of layers is somewhat subjective

 CCC 1022-1360/00/$ 17.50+.50/0

anyway. The "skin region" is often considered to be very thin and essentially having a relatively high amorphous content due to rapid cooling. The lower cooling rate in the "core region" can allow complete relaxation of the chain molecules and the growth of spherulites. A "shear zone" generally separates the skin and core regions. The thickness of these regions can be different, depending on the position and the conditions of injection moulding.

In the following, some results of experiments characterising the morphology of polypropylene injection mouldings are presented, and the results discussed in terms of the histories involved.

Experimental

Two different polypropylenes have been used, Solvay Eltex PHV252, an isotactic polypropylene homopolymer (iPP), and Montell Australia ZMA 6170 PP, a nucleated copolymer polypropylene (cpPP) injection moulding grade with a melt index of 60. These were injected under a variety of conditions, and the morphologies characterised using x-ray scattering experiments at the Australian National Beamline Facility (ANBF) at the Photon Factory in Tsukuba, Japan.

The rectangular mould cavity used for the iPP was 200mm long, 40mm wide and 4.5mm deep. It had a fan gate opening through a 2mm slot across the 40mm end. Only one set of moulding conditions was used, with a melt temperature of 230°C, mould temperature 45°C, and filling time 2.2s.

The rectangular mould cavity used for the cpPP was 78mm long, 40mm wide and 3mm deep, with a central gate opening through a rectangular 1.5mm by 3mm slot centrally into the 40mm end. The mould temperature was 80°C and the melt temperature 180°C, and in this case several injection rates were used.

The end-gated geometries were chosen to ensure a relatively straight non-divergent flow front during the filling process, particularly in the centre where most results have been obtained. Wide-angle x-ray scattering (WAXS) and small-angle x-ray scattering (SAXS)

were simultaneously recorded using a line-shaped beam with a vertical height of 100μm and width 0.8mm. Monochromatic radiation with a wavelength of either 0.20nm or 0.157nm was used. The illuminated zone was changed with a vertical shift of the sample holder in steps of either 200μm or 300μm and intensities were registered in the range of scattering angles 2θ from 0.0016 to 35 degrees.

Measurements were performed with the primary beam being perpendicular to the flow direction, the scattering being measured along a direction normal to the layers in the moulding. Physical parameters calculated later will be plotted as a function of the depth in the direction of the plate thickness. The first measurement was taken with the beam centre 100μm from the surface, but should not be taken as a measurement of the skin as the x-ray beam cannot access the specimen skin in the present experiments. In the quantitative evaluation of WAXS data, the background due to the amorphous contribution was determined by fitting a polynomial to a number of chosen points of each curve and subsequently subtracting this from the measured data.

The degree of volume crystallinity, x_v, can be determined from WAXS data using a method proposed by Ruland[4]. The basis of this method is that if the scattered intensity can be separated into crystalline and amorphous contributions, the crystalline fraction can be defined as the ratio of the crystalline scattering $I_c(q)$ to the total scattered intensity $I(q)$, these intensities being integrated over all values of the scattering vector q ($q = 4\pi\sin\theta/\lambda$ for scattering angle 2θ and radiation wavelength λ). The other key element to Ruland's proposal is that this ratio must also be corrected to allow for crystalline imperfection due to thermal and other sources. This method has a sound physical basis and x_v is considered to be an absolute degree of volume crystallinity.

The procedure has since been modified by Vonk[5] to allow for integration of intensities over the finite range of scattering vector experimentally available, and simplified by assuming a particular q dependence of the imperfection. The resultant equation defining the volume crystallinity is

$$x_v \approx \frac{\int_{q_l}^{q_u} q^2 I_c(q)dq}{\int_{q_l}^{q_u} q^2 I(q)dq}(1+kq_u^2/2) = \frac{(1+kq_u^2/2)}{R(q_u)} \quad (1)$$

where k is a measure of imperfection (the imperfection factor), q_l and q_u are the lower and upper limits of integration, and $R(q_u)$ is defined by the equation for a fixed value of q_l.

The absolute degree of the volume crystallinity x_v and the imperfection factor k of the crystalline regions can be obtained from a linear least-square fitting of $R(q_u)$ versus q^2_u. At lower values of q_l, there is an oscillation of $R(q_u)$ with increasing q_u, and so in the regression analysis, the upper limit q_u was fixed and the fitting was executed at different values of the lower limit q_l until a constant x_v was achieved.

An alternative measure of crystallinity based on a ratio of peak heights has also been proposed[6], which has the advantage of being easier to routinely calculate. This crystallinity index is defined as[6]

$$C = \frac{h_{\alpha 1} + h_{\alpha 2} + h_{\alpha 3} + h_{\alpha 4} + h_\beta}{5h_a} \quad (2)$$

where $h_{\alpha 1}$, $h_{\alpha 2}$, $h_{\alpha 3}$, $h_{\alpha 4}$ and h_β, are the heights of the the various α and β crystalline peaks, and h_a the height of the amorphous peak. It should be pointed out that such a crystallinity index determined from the peak heights of WAXS data is not directly related to the fraction of the crystalline phase of bulk materials and cannot be physically compared with the degree of the crystallinity obtained from the other methods such as differential scanning calorimetry and density measurement.

Results using both methods of crystallinity determination discussed above are presented in the following section.

To characterise the amount of β phase present, a β index was used, this also being based on a ratio of peak heights. This has been defined[6] as

$$B = \frac{h_\beta}{h_{\alpha 1} + h_{\alpha 2} + h_{\alpha 3} + h_\beta} \quad (3)$$

where $h_{\alpha 1}$, $h_{\alpha 2}$, $h_{\alpha 3}$ and h_{β}, are the heights of the the various α and β crystalline peaks.

Results and Discussion

Optical microscopy of the mouldings using crossed polars shows features typical of injection moulded articles, with a clear layered structure with the layers parallel to the adjacent surface. The iPP comprised large spherulites (around 50 μm) both near the surface and in the central region, separated by a relatively featureless region. Also a number of bright spherulites were evident in the outer layers, presumably due to the highly birefringent β phase. The cpPP moulding showed a much finer crystalline structure, with spherulites being of order 10 μm in diameter.

Figure 1 shows the distribution of volume crystallinity through the thickness direction for both the polypropylenes. Clearly the crystallinity varies significantly in the iPP through the thickness, and is higher toward the surface both near the gate and in the central region.

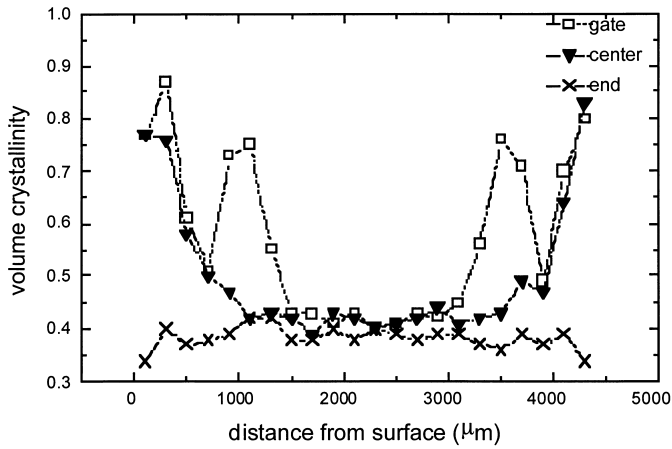

Figure 1(a) Volume crystallinity distribution in the iPP at three positions in the 4.5mm thick cavity moulding (calculated using Ruland's method[4,5] to give an actual crystallinity).

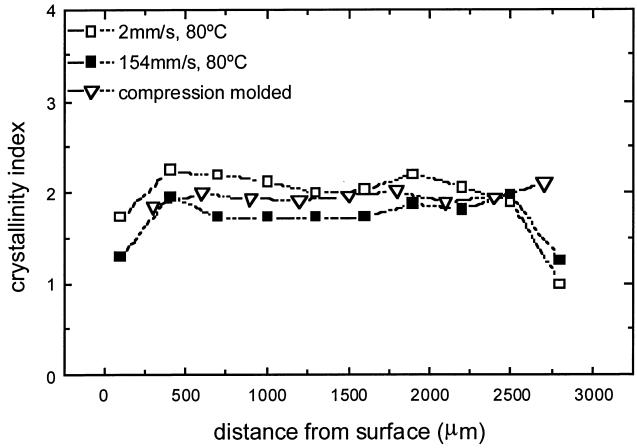

Figure 1 (b) Crystallinity distribution[6] through the central region of cpPP 3mm thick cavity mouldings (from a comparison of crystalline and amorphous peaks) for a fast and slow injection speed, and a 3mm thick compression moulding.

A flat distribution is seen near the end. Near the gate the distribution shows multiple peaks, which matches with optical observations of a five layered structure in each half thickness, thought to be due to the primary flow during the filling stage being followed by a secondary phase of slower flow during the packing stage. In contrast, the crystallinity in the cpPP is roughly constant through the moulding, with a decrease near the surface. Within experimental error, the level of crystallinity in the cpPP is also independent of moulding speed (and thus shear rate), and is the same as obtained in a compression moulded sample of the cpPP. For purposes of comparison, a volume crystallinity of 0.4 for the iPP corresponds to a crystallinity index of 2.3, showing that the base levels of crystallinity in the two polypropylenes are comparable.

Figure 2 shows the distribution of ß-phase through mouldings of both polymers, where a distinct peak in the concentration of the hexagonal ß-phase just below the surface is evident. The concentration of the ß-phase near the surface and in the core region drops to

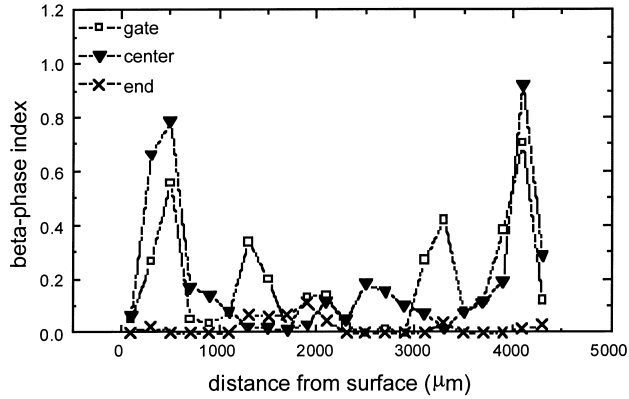

Figure 2 (a) The distribution of beta phase[6] PP crystalline form through the 4.5mm thick cavity iPP moulding at three different regions.

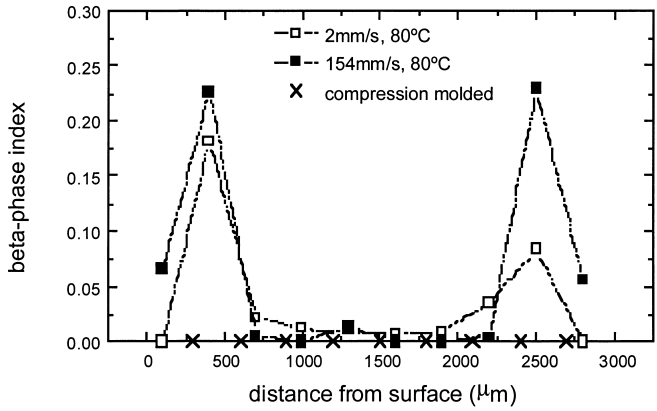

Figure 2 (b) The distribution of beta phase[6] PP crystalline form through the central region of two cpPP 3mm thick cavity mouldings, and a 3mm thick compression moulding.

a small value, but not to zero as found for a compression-moulded sample (figure 2 (b)). In addition, figure 2(b) shows a larger amount of β phase at the higher injection speed,

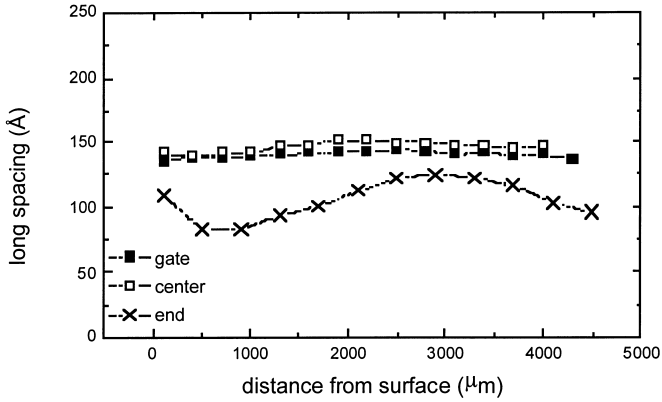

Figure 3 (a) The distribution of long spacing calculated from the SAXS data[7] for the 4.5mm thick cavity iPP moulding.

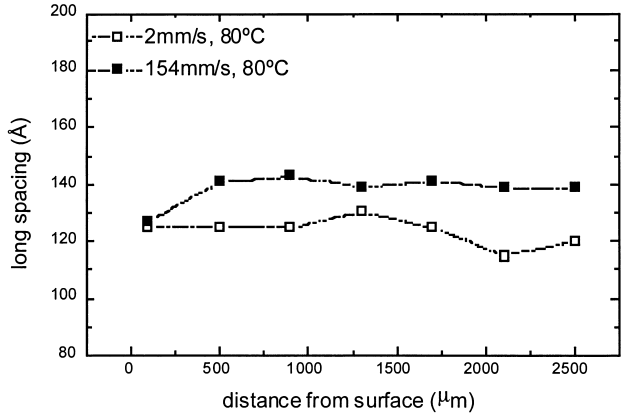

Figure 3 (b) The distribution of long spacing calculated from the SAXS data[7] for two 3mm thick cavity mouldings of cpPP.

most likely due to the higher shear rate generated. Also, a second pair of peaks in the concentration of β phase is observed in the iPP near the gate, reflecting the shear during the packing phase, as discussed above. Figure 3 shows the long spacing calculated from the SAXS. It shows a lower long spacing at the end of the iPP moulding, but the essentially constant long spacing at the other sites does not vary in any way to reflect the significant variations in crystallinity evident from figure 1 (a).

Figures 4 and 5 show the Moldflow MPI simulated shear rate distribution and temperature distribution across the sample thickness at the middle of the moulding at the end of the filling stage. The simulation results discussed here were done for the iPP mouldings, but the results for the cpPP show the same trends and similar magnitudes of shear stress and temperature. The highest shear rate at the midpoint of the moulding

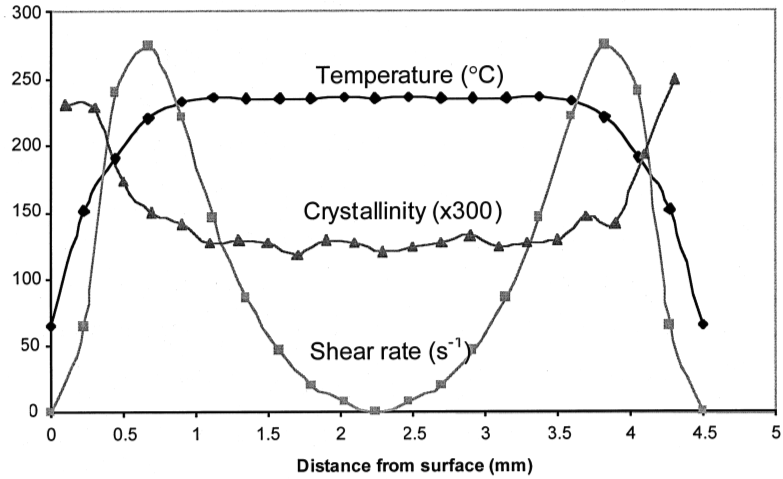

Figure 4 Temperature and shear rate distribution through the thickness of the 4.5mm thick cavity predicted by Moldflow MPI for the iPP at the end of the filling stage compared with the crystallinity distribution (from figure 1(a)) measured using x ray diffraction

occurs at the point around 0.3 half-thickness away from the surface.

Also shown on figure 4 is the crystallinity distribution at the middle of the moulding,

taken from figure 1(a). It can be seen that the higher crystallinity observed near the surface corresponds to the region where the temperature at the end of the filling stage is somewhat lower than the melt temperature, and the shear rate is appreciable.

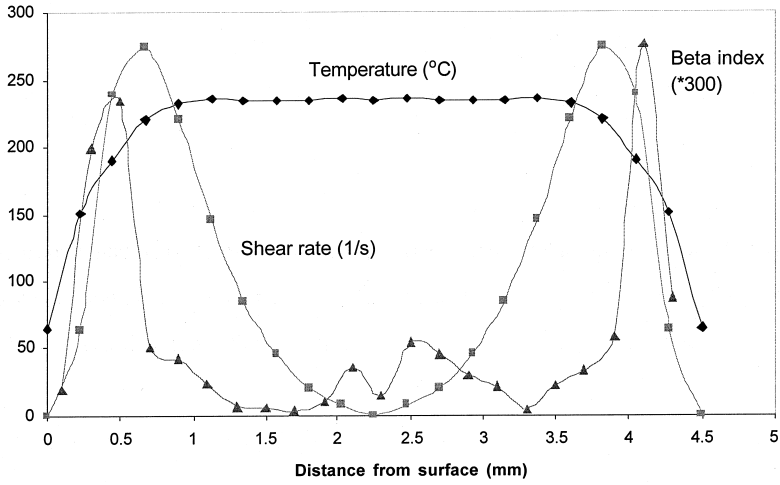

Figure 5 Temperature and shear rate distribution through the thickness of the 4.5mm thick cavity predicted by Moldflow MPI for the iPP at the end of the filling stage compared with the β phase distribution (from figure 2(a)) measured using x ray diffraction.

The morphology developed in an injection moulding of course depends on the history of shear and temperature, and not simply the conditions at the instant of mould filling. In that sense, figures 4 and 5 are incomplete, as solidification takes place both before and after the mould is filled. To take this into account, an attempt was made to estimate the thermal and shear history of representative points in the final moulding by using a simple 'back-tracking" model in conjunction with MPI. The main assumption of the backtracking model is that the polymer particles flow horizontally. Due to fountain flow at the melt front, this assumption is not true for polymer particles that end up in the vicinity of the mould wall, but is reasonable for polymer particles away from the edge of the moulding.

For a specific polymer particle, at a specific time step, its velocity, temperature, and shear rate can be estimated using Moldflow MPI simulation. By assuming that the polymer particle travels from a previous time step to the current time step at the current velocity, the location of the polymer particle at the previous time can be predicted. Once the location of the polymer particle in the previous time step is determined, Moldflow MPI can be used to identify its velocity, temperature, and shear rate, by simulating a short shot. If the velocities at the previous and current time steps differed by more than 5%, an iterative procedure, using a velocity averaged over the time step to do the particle back tracking, until the velocity difference between the two times was less than 5%, was followed. By using this simple model, the thermal and shear histories of specified polymer particles can be identified.

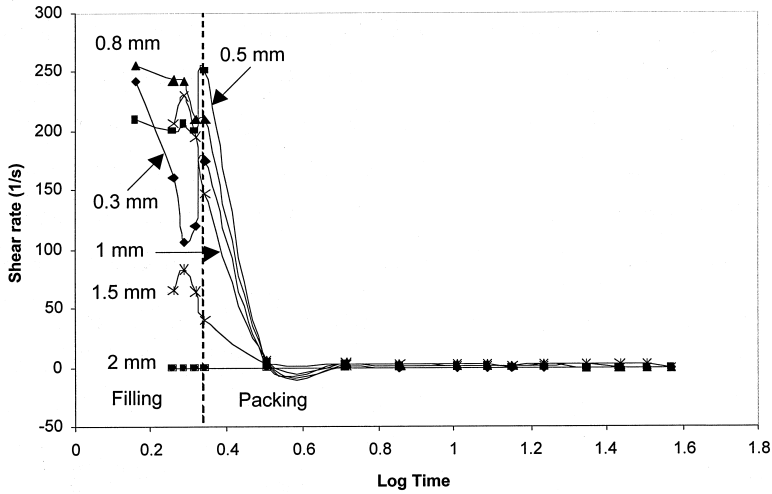

Figure 6 Shear histories of a number of points at the central developed flow region of an iPP moulding at various (labelled) distances from the surface of the ~4.5mm thick moulding. (Time is measured in seconds).

Figures 6 and 7 show the shear rate and temperature histories predicted by this procedure for a range of polymer particles which at the end of filling were at the given distances

from the surface in the central region of the moulding, midway between the gate and the end. The times at which the stresses and temperatures were estimated during the filling stage correspond to the mould being 64%, 80%, 87%, 95% and 100% filled, the time being measured from the commencement of injection. The filling time for this particular set of moulding conditions is 2.2s. During the packing stage directly after filling, stresses and temperatures were calculated for a sequence of times up to 36s after injection commenced. The simulation software changes from flow rate boundary conditions appropriate to the filling stage to pressure boundary conditions suitable for the packing stage at a preset time just before the mould is filled.

Some of the faster moving central particles could not be backtracked to the 64% fill stage, as they were predicted to be in the gate or runner at this time.

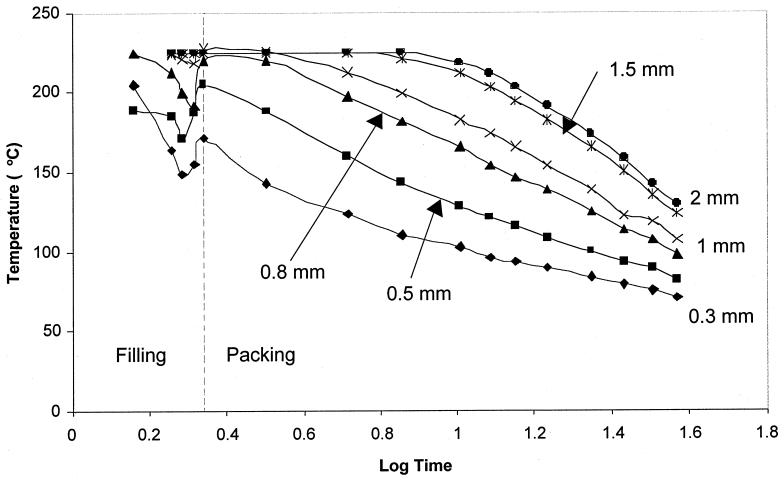

Figure 7 Temperature histories of a number of points at the central developed flow region of an iPP moulding at various (labelled) distances from the surface of the ~4.5mm thick moulding. (Time is measured in seconds).

Figure 6 suggests that the region between 0.5mm to around 1mm away from the surface experiences the highest shear in the latter stages of processing. Regions further from the

surface than this are in the central low-shear flow regime, whereas the regions outside this (less than 0.3mm) are already in the solidified layer. The increase of shear rates at the time near the end of filling is due to the switchover from a flow rate boundary condition to a pressure boundary condition before the cavity is completely filled. Figure 7 indicates that the cooling rate increases closer to the surface as expected, but also that the temperature in the outer regions may increase near the end of the mould filling stage. This could be due to shear heating and compression heating effects, but the laminar flow assumption of the backtracking model breaking down near the surface is also a possible explanation.

The region of high shear and rapid cooling corresponds to the region of increasing crystallinity (see figure 1 (a)) and the peak in β phase content (see figure 2 (b)) in the iPP mouldings. In the case of the cpPP material, simulation gives very similar shear and temperature profiles at the instant of filling to the iPP simulation, but the crystallinity has no maximum in the high shear region (see figure 1 (b)), rather it decreases slightly toward the surface. It seems that shear induced crystallisation of the α phase which evidently occurs in the iPP is overshadowed by the nucleating agent in the cpPP polymer compound. In contrast, the β phase concentration in the cpPP has distinct maxima in the high shear regions adjacent to the surfaces, indicating that shear induced formation of β crystallites still occurs in this nucleated material.

It can be seen from figures 4 (or 5) and 7 that at the end of the filling stage a large proportion of the central region of the moulding is above the melting temperature of the iPP (~ 170 °C), and solidification will obviously continue beyond this stage, emphasising the importance of monitoring the history of material points in some way.

Conclusions

A correspondence between processing history and resultant morphology in polypropylene has been demonstrated, but it is also clear that any relationship must be

material and grade specific. Although shear rate and temperature history can strongly influence the morphology of the polymer throughout the moulding, factors such as the presence of a nucleating agent can be significant.

[1] Kantz M R, Newman JR, and Stigale F H, **1972** *J. applied polymer science* 16, 1249-1260.
[2] Fitchmun D R, Mencik Z, **1973** *J. polymer science: polymer physics edition* 11, 951-971.
[3] Wenig W, Herzog F., **1993** *J. applied polymer science* 50, 2163-2171.
[4] W. Ruland, **1961** *Acta Cryst.* 14, 1180.
[5] C. G. Vonk, **1973** *J. Appl. Cryst.* 6, 148
[6] J. P. Trotignon, J. L. Lebrun, J. Verdu, **1982** *Plastics Rubber Process Applicat.* 2, 247.
[7] G. R. Strobl, **1997** "*The physics of polymers*", Springer, New York